JOURNAL OF AGRICULTURAL AND FOOD CHEMISTRY

Article

pubs.acs.org/JAFC

Cell Wall, Cell Membrane, and Volatile Metabolism Are Altered by Antioxidant Treatment, Temperature Shifts, and Peel Necrosis during Apple Fruit Storage

Rachel Leisso, David Buchanan, Jinwook Lee, James Mattheis, and David Rudell*

Tree Fruit Research Laboratory, Agricultural Research Service, U.S. Department of Agriculture, 1104 North Western Avenue, Wenatchee, Washington 98801, United States

ABSTRACT: The transition from cold storage to ambient temperature alters apple quality through accelerated softening, flavor and color changes, and development of physiological peel disorders, such as superficial scald, in susceptible cultivars. To reveal global metabolism associated with this transition, the 'Granny Smith' peel metabolome was evaluated during storage of 6 months and shelf life periods. Treatment with the antioxidant diphenylamine (DPA) reduced scald, creating a metabolic contrast with untreated fruit, which developed superficial scald. Superficial scald symptoms developed on control fruit after 120 days of storage, and symptoms progressed following transition to ambient-temperature shelf life. The metabolic profile of control and DPA-treated fruit was divergent after 30 days of cold storage due to differing levels of α-farnesene oxidation products, methyl esters, phytosterols, and other compounds potentially associated with chloroplast integrity and oxidative stress response. Hierarchical cluster analysis revealed coregulation within the volatile synthesis pathway including control of the availability of methyl, propyl, ethyl, acetyl, and butyl alcohol and/or acid moieties for ester biosynthesis. Overall, the application of metabolomics techniques lends new insight into physiological processes leading to cell death and ripening processes that affect fruit flavor, appearance, and overall quality.

KEYWORDS: *superficial scald, antioxidant, diphenylamine, volatile aroma esters, shelf life, ripening*

INTRODUCTION

The pitted and necrotic peel lesions that characterize the peel disorder of apple fruit known as superficial scald are thought to result from oxidative stress caused by chilling injury. Superficial scald symptoms typically appear after approximately 2 months of cold storage and can worsen during shelf life following removal from cold storage, although compounds associated with the disorder increase early in storage, prior to symptom development.[1] These compounds include oxidative products of α-farnesene, specifically conjugated trienols including 2,6,10-trimethyldodeca-2,7(*E*),9(*E*),11-tetra-6-ol (CTol), 6-methyl-5-hepten-2-one (MHO), and 6-methyl-5-hepten-2-one (MHol).[2] Treatment with the antioxidant diphenylamine (DPA) can ameliorate or prevent scald symptoms in part by preventing the oxidation of α-farnesene and other effects of oxidative stress.[1] Additional known effects of DPA treatment on apple fruit include changes in volatile compounds contributing to aroma,[3] ethylene production,[4] and respiration rate.[5] Although the disorder is attributed to oxidative stress, the exact metabolic processes surrounding injury development are not well-characterized.

Major biochemical changes in 'Granny Smith' apple peel related to superficial scald development during cold storage (1 °C) have been described using untargeted metabolic profiling.[6] Yet, whereas the effects of ambient temperature (20 °C) shelf life have been detailed with respect to volatile aroma production,[3] shelf life dynamics are often limited to a few time points, and additional metabolites have often been targeted to single or small groups of metabolites such as lipids and fatty acids[8] and nitrogenous compounds.[9] The greater metabolic phenotype associated with progressive superficial scald symptom development during shelf life is uncharacterized and may lend insight to the nature of injury inception and progression. Metabolic profiling can delineate processes and pathways associated with a particular phenotype[10−12] and has been utilized to demonstrate the complex effects of postharvest treatments on particular metabolites or groups of metabolites in the apple peel metabolic profile.[6]

The goal of this work was to characterize the changes to the 'Granny Smith' apple peel metabolic profile induced by antioxidant treatment, cold storage, and warm-temperature shelf life in relation to superficial scald development using metabolic profiling techniques and a combination of univariate and multivariate data analyses.

MATERIALS AND METHODS

Plant Material, Treatments, Storage Conditions, and Superficial Scald Symptom Evaluation. 'Granny Smith' apples (*Malus sylvestris* L. (Mill.) var. *domestica* Borkh. Mansf. cv. Granny Smith) were treated with 2 g L^{-1} DPA (Sigma-Aldrich, St. Louis, MO, USA) or equal concentrations of carrier and surfactant (control fruit)[6] and stored for 180 days at 0.5 °C. At 30, 60, 120, and 180 days, three trays (18 fruits per tray) were removed to 20 °C. Superficial scald was rated immediately after removal from cold storage as well as after 7 and 14 days at 20 °C (Figure 1). Superficial scald symptom development was rated using an index of 1−4 with 1 = none, 2 = <25%, 3 = 25−50%, or 4 = >50% of the peel surface having superficial scald symptoms. One tray (18 fruits per tray) was peeled at each evaluation time; three fruits

Received: October 29, 2012
Revised: January 10, 2013
Accepted: January 13, 2013
Published: January 13, 2013

dx.doi.org/10.1021/jf3046208 | *J. Agric. Food Chem.* 2013, 61, 1373−1387

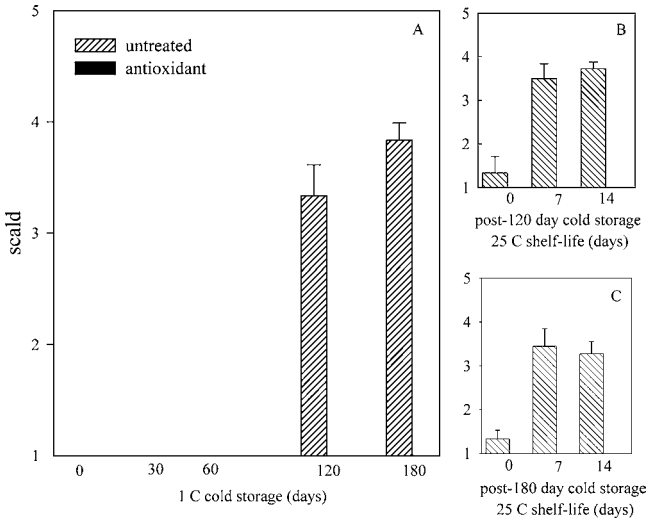

Figure 1. Final scald incidence and severity following shelf life increased between 120 and 180 days of cold storage (A); scald incidence and severity also increased following removal from cold storage (day 0) during shelf life (days 7 and 14) and at 120 days (B) and 180 days (C) of storage. Scald symptoms were rated 1−4 (1 = no scald, 2 = 0−25%, 3 = 25−75%, 4 = ≥75%). No symptoms were apparent in either treatment prior to 120 days of storage.

were peeled into one sample cup for a total of six samples. Peel samples were collected by peeling five longitudinal strips from each fruit, followed by immediate immersion in liquid nitrogen. Frozen peel was cryogenically milled to a fine powder and stored at −80 °C prior to metabolite analysis.

Metabolite Extraction and Evaluation. *Tissue Processing.* Frozen peel powder was analyzed using three extraction procedures and four instrumental analyses to evaluate the metabolome:

1. Trimethylsilyl(oxime) Derivative Analysis. Methanolic extraction coupled with trimethylsilyl(oxime) derivatization and GC-MS analysis of frozen apple peel powder (0.1 g) was conducted as previously described.[6]

2. Volatile Metabolite Analysis. Frozen peel powder (0.5 g) was weighed into 20 mL glass headspace vials (Gerstel, Baltimore, MD, USA) previously chilled in N_2(l). Vials containing sample were removed from N_2(l), 1 mL of saturated NaCl solution and 10 μL of an aqueous internal standard mixture containing 34.4 ng μL^{-1} 1-methylethyl butyrate (Aldrich Chemical Co., Milwaukee, WI, USA) and 33.4 ng μL^{-1} 5-hexanol (Sigma-Aldrich, St. Louis, MO, USA) were added, and then the vials were sealed. Vials were incubated at 22 °C for 5 min and then sonicated at 25 °C in an ultrasonic bath for 5 min prior to headspace analysis.

Vial headspace was analyzed using an Agilent 6890N gas chromatograph coupled with a 5975B mass selective detector (Agilent Technologies, Palo Alto, CA, USA) and an automated Gerstel multipurpose sampler (MPS) equipped with a dynamic headspace sampler (DHS). Headspace vial temperature was maintained at −1 °C using a cooled sample tray until sampling. At the beginning of the headspace sampling sequence, vials were vortexed at 1000 rpm during incubation at 30 °C for 10 min prior to sampling. To sample, analyte was collected by sweeping 220 mL of He at 20 mL min^{-1} through the headspace, and then a 60 mm (length) × 6 mm (o.d.) glass tube (trap) containing 90 mg of Tenax TA (60/80 mesh) and 60 mg of Carbosieve 3 (60/80 mesh) (Supelco, St. Louis, MO, USA) maintained at 30 °C. After loading, water was removed from the trap by sweeping the sorption bed with 400 mL of He at 40 mL min^{-1} while the trap was heated to 35 °C.

Traps were desorbed at 20 mL min^{-1} with the inlet set in the solvent purge mode and purge pressure adjusted to the inlet pressure. The desorption temperature program started at 30 °C for 0.2 min, increased at 720 °C min^{-1} to 300 °C, and then held for 3 min. Desorbed analyte was collected on a glass bead-filled liner maintained at −145 °C for the entire desorption period.

Analyte was introduced into the GC column (HP-5MS, Agilent) (30 m × 250 μm × 0.25 μm) by heating the liner to 150 °C at 16 °C s^{-1} and then to a final temperature of 300 °C at 12 °C s^{-1} held for 3 min. The He carrier linear velocity was 40 cm s^{-1}, and the injection split ratio was 1:5; the initial oven temperature was 30 °C for 0.5 min and then increased to 300 °C at 12 °C min^{-1}. The detector was operated in the electron impact mode with transfer line, source, and quadrupole temperatures maintained at 250, 150, and 230 °C, respectively. Mass spectra ranging from m/z 30 to 600 were recorded.

3. LC-MS Evaluation. Frozen peel powder (0.5 g) was weighed into 2 mL opaque, screw-top microcentrifuge tubes previously chilled in N_2(l) to which ∼100 μL of 0.5 mm (diameter) soda lime glass beads (BioSpec Products, Inc., Bartlesville, OK, USA) was added. Tubes were placed at room temperature, and 100 μL (79.8 ng μL^{-1}) of α-tocopherol acetate (Sigma-Aldrich, St. Louis, MO, USA) internal standard followed by 0.71 mL of 2:1 acetone/0.2 M HEPES, pH 7.7, was added, and the tubes were centrifuged at 2000g for 15 s. Then another 0.71 mL of acetone/HEPES was added, after which the tubes were shaken vigorously for 1 min using a Mini Beadbeater (BioSpec Products, Inc.) and then centrifuged at 16200g for 1 min. The supernatant was transferred to a 13 × 100 mm borosilicate test tube (stored in the dark and on ice) using a borosilicate pipet. The pellet was washed twice by adding 1 mL of acetone (Fisher Scientific, Fair Lawn, NJ, USA), bead beating the sample for 30 s, and then centrifuging the mixture as described above. The pellet was then washed with 0.75 mL of hexanes (Fisher Scientific) and the supernatant transferred to the test tube containing the compiled buffered acetone extract. The test tube was vortexed for 15 s, and the hexanes phase transferred to a clean test tube after the phases separated. Another 0.75 mL of hexanes was added directly to the extract, vortexed, and allowed to separate while the tubes were held on ice before the hexanes phase was transferred to the collection tube. This step was repeated once. The hexanes phase was dried under a stream of N_2(g), the residue dissolved in 250 μL of acetone, and the sample filtered using a 0.45 μm PTFE syringe filter prior to analysis.

Samples were analyzed by injecting 10 μL into a series 1100 HPLC system (Agilent Technologies) controlled by Chemstation (B.02.01) and equipped with a Chromolith Performance RP-18e (4.6 × 100 mm) monolithic reverse-phase column (EMD Chemicals, Inc., Gibbstown, NJ, USA), a G1315B diode array detector, and a G1946D single-quadrupole mass selective detector using an atmospheric pressure chemical ionization (APCI) source. Elution solvents used for a linear gradient were (A) 80:20 methanol/deionized water and (B) ethyl acetate (Fisher Scientific). The column temperature and mobile phase flow rate were 20 °C and 1.0 mL min^{-1}, respectively. The mobile phase was composed entirely of solvent A for the initial 2 min after sample injection, followed by a linear gradient of solvent A plus B to 65% B at 21 min and then entirely solvent B until 35 min. The eluate was first analyzed by the DAD and then the MSD. The DAD continuously monitored and recorded spectra (190−700 nm) for the entire analysis.

The APCI spray chamber conditions were as follows: drying gas (N_2) flow, 4 L min^{-1}; drying gas temperature, 350 °C; nebulizer pressure, 414 kPa; vaporizer temperature, 425 °C; and coronal discharge, 4 μA. The fragmentor and capillary potentials were 170 and 4000 V, respectively. The MSD was adjusted to monitor positive ions in the scanning mode within a m/z 100−1200 range.

Data Acquisition, Deconvolution, and Peak Identification. User-defined GC-MS and LC-MS libraries were generated using the automated mass spectral deconvolution and identification system (AMDIS; National Institute of Standards, Gaithersburg, MD, USA) to find unique components within the chromatographic mass spectral data. For GC-MS data, retention indices (RI) were generated for each sequence by comparing the retention times of C10−C40 hydrocarbons evaluated under the same conditions as the samples with the retention times of sample components. From libraries constructed by evaluation of AMDIS search results of samples from each treatment at the extremes of storage duration and shelf life, mass spectral tags

Table 1. Metabolite Levels in Apple Fruit Peel Were Extracted According to Three Procotols [(A) Volatile Head Space, (B) Methanolic Extraction and TMS Derivitization, and (C) Acetone Extraction], Followed by Assessment of Relative Levels on GC-MS (for A and B) and LC-MS (C) Instrumentation[a]

(A) Volatile Headspace Extraction; GC-MS

metabolite	abbrev	mass spectral tag (retention index, target ion)	coelution standard source	metabolite	abbrev	mass spectral tag (retention index, target ion)	coelution standard source
(*E*)-2-heptenal	2-Hept	961.5, 83	Sigma-Aldrich[b]	ethanol	EtOH	526.3, 45	
(*E*)-2-octenal	2-Oct	1071.0, 83	Sigma-Aldrich	ethyl 2-methylbutanoate	E-2MBut	851.3, 57	Sigma-Aldrich
(*E*)-2-hexenal	2-Hex	855.6, 98	Sigma-Aldrich	ethyl acetate	EAce	617.5, 88	Sigma-Aldrich
(*E*,*E*) -2,4-hexadienal	2,4Hex	914.8, 81	Sigma-Aldrich	ethyl butanoate	EBut	805.1, 43	Sigma-Aldrich
(*E*,*E*)-α-farnesene	(E,E)a-farn	1509.5, 119.1	purified/extracted[c]	ethyl hexanoate	EHex	999.3, 88	Sigma-Aldrich
(*Z*)-2-hexen-1-ol	2-Hex-1	869.4, 57	Sigma-Aldrich	ethyl pentanoate	EPen	902.3, 85	Sigma-Aldrich
(*Z*)-3-hexen-1-ol	3-Hex	854.4, 82	Sigma-Aldrich	ethyl propanoate	EPro	718.5, 57	Sigma-Aldrich
(*Z*,*E*)-α-farnesene	(Z,E)a-farn	1496.6, 93	purified/extracted[c]	heptanal	HepAl	903.3, 43	Sigma-Aldrich
1-butanol	1-But	672.8, 56	Sigma-Aldrich	hexanal	HexAl	804.9. 41	Sigma-Aldrich
1-hexanol	1-Hex	871.8, 56	Sigma-Aldrich	hexyl 2-methylbutenoate	H-2MButen	1331.2, 109	Sigma-Aldrich
1-pentanol	1-Pen	772.4, 42	Sigma-Aldrich	hexyl 2-methylbutyrate	H-2MBut	1235.8, 103	Sigma-Aldrich
1-propanol	1-Pro	583.3, 31	Sigma-Aldrich	hexyl acetate	HAce	1013.2, 43	Sigma-Aldrich
2-butanol	2-But	616.2, 45	Sigma-Aldrich	hexyl butanoate	HBut	1190, 99	Sigma-Aldrich
2-methyl-1-butanol acetate	2-MBAce	880.3, 70.1	Sigma-Aldrich	hexyl hexanoate	HHex	1383.8, 117.1	Sigma-Aldrich
2-methyl-1-propanol	2-MP	629.3, 43.1	Baker[d]	hexyl pentanoate	HPen	1287.3, 85.1	synthesized[e]
2-methylbutanol	2-MB	741.9, 57.1	Sigma-Aldrich	hexyl propanoate	HPro	1104.2, 57	Sigma-Aldrich
2-methylbutylhexanoate	2-MBHex	1254.8, 99	synthesized[e]	methoxybenzene	MxBenz	902.2, 108	Sigma-Aldrich
2-methylpropylbutanoate	2-MPBut	956.4, 71	synthesized[e]	methyl 2-methylbutyrate	M-2MBut	781.7, 88	Sigma-Aldrich
(*E*)-2-pentenal	2-Pent	759.5, 83.1	Alfa Aesar[f]	methyl 2-methylpropanoate	M-2MPro	687, 71	synthesized[e]
2-propanol	2-Pro	531.60, 45	Fisher[g]	methyl acetate	MAce	532.6, 74	Sigma-Aldrich
6-methyl-5-hepten-2-ol	6MHol	994.5, 95	Sigma-Aldrich	methyl alcohol	MeOH	491.60, 31.1	Fisher
6-methyl-5-hepten-2-one	6MHO	988.4, 55	Sigma-Aldrich	methyl butanoate	MBut	729.2, 74	Sigma-Aldrich
acetaldehyde	AcetAld	471, 44	Fisher	methyl hexanoate	MHex	925.4, 74	Sigma-Aldrich
acetic acid	AcA	706.2, 60	Mallinckrodt[h]	methyl propionate	MPro	632.8, 57	Sigma-Aldrich
acetone	Ace	509.5, 58	Sigma-Aldrich	nonanal	Non	1116, 57	Sigma-Aldrich
benzaldehyde	Benz	965.6, 106	Sigma-Aldrich	pentanal	PenAl	701.9, 44	Sigma-Aldrich
β-farnesene	B-farn	1457.1, 69	TCI[i]	pentyl butyrate	PBut	1093.4, 71	Sigma-Aldrich
butyl 2-methylbutyrate	B-2MBut	1041.9, 57	Sigma-Aldrich	pentyl hexanoate	PHex	1286.3, 117	Sigma-Aldrich
butyl acetate	BAce	817.6, 43.1	Sigma-Aldrich	pentyl acetate	PAce	914.9, 70	Sigma-Aldrich
butyl butyrate	BBut	995.7, 71	Sigma-Aldrich	propyl butanoate	PrBut	899.4, 71	Sigma-Aldrich
butyl hexanoate	BHex	1190, 99	synthesized[e]	propyl hexanoate	PrHex	1094, 99	Sigma-Aldrich
butyl propanoate	BPro	909.4, 57	synthesized[e]	propyl propionate	PrPro	813.0, 57	Sigma-Aldrich
4-allylanisole	Est	1202.4, 148	Sigma-Aldrich				

(B) Methanolic Extractions and TMS Derivatization

metabolite	abbrev	mass spectral tag (retention index, target ion)	coelution standard source	metabolite	abbrev	mass spectral tag (retention index, target ion)	coelution standard source
(−)-epicatechin	Epicat	2886.2, 368.2	Sigma-Aldrich	L-homoserine	HSer	1456.3, 218.2	Sigma-Aldrich
(±)-catechin	Cat	2905.9, 368.2	Sigma-Aldrich[k]	hydroxyproline	HyPro	1530.6, 230.2	Sigma-Aldrich
1-aminocyclopropane-1-carboxylic acid	1-ACC	1216.9, 202.2	Sigma-Aldrich	hyperin	Hyp	3719.8, 217.1	Indofine
2-oxoglutaric acid	2-OgA	1579.6, 198	Sigma-Aldrich	*myo*-inositol	Ino	1832.7, 273.1	Sigma-Aldrich
5-oxoproline	5-OPro	1529.70, 156	Sigma-Aldrich	L-isoleucine	Ile	1296.7, 158.2	Sigma-Aldrich
γ-aminobutyric acid	GABA	1535.5, 304.2	Sigma-Aldrich	L-leucine	Leu	1276.5, 158.1	Sigma-Aldrich
adonitol	Ado	1745.2, 217.1	Sigma-Aldrich	linoleic acid	Lin	2210.7, 337.1	Sigma-Aldrich
L-alanine	Ala	112.0, 116	Sigma-Aldrich	maleic acid	MaleA	1307.9, 245.1	Sigma-Aldrich
asparagine	Asn	1601.2, 116.1	Sigma-Aldrich	malic acid	MalA	1495, 335.2	Sigma-Aldrich
L-aspartic acid	Asp	1524.8, 232.2	Sigma-Aldrich	malonic acid	MaloA	1208.6, 233.1	Fisher
β-alanine	B-Ala	1432.2, 248	Sigma-Aldrich	mucic acid	MucA	2079.2, 333.2	Fluka
chlorogenic acid	ChA	3146.77, 345.2	Sigma-Aldrich	norvaline	Nor	1241, 144.2	Sigma-Aldrich
citramalic acid	CitMA	1482.4, 247.1	Sigma-Aldrich	phenylalanine	Phe	1555.8, 218	Sigma-Aldrich
citric acid	CitA	1840, 273.1	Sigma-Aldrich	phloridzin	Phl	3510, 342.1	Sigma-Aldrich
dodecanoic acid	DoDecA	1648.8, 257.2	Sigma-Aldrich	phosphoric acid	PhoA	1279.9, 299.1	J. T. Baker
eicosanoic acid	EicA	2434.5, 369.2	Sigma-Aldrich	pipecolic acid	PipA	1370.9, 156.1	Sigma-Aldrich

dx.doi.org/10.1021/jf3046208 | J. Agric. Food Chem. 2013, 61, 1373−1387

Table 1. continued

(B) Methanolic Extractions and TMS Derivatization							
metabolite	abbrev	mass spectral tag (retention index, target ion)	coelution standard source	metabolite	abbrev	mass spectral tag (retention index, target ion)	coelution standard source
erythritol	EryOl	1517.3, 217.1	Sigma-Aldrich	L-proline	Pro	1529.7, 156.1	Sigma-Aldrich
erythrose	Ery	1463.3, 205.1	Fluka[l]	pyruvic acid	PyrA	1060.9, 174.1	Sigma-Aldrich
fructose	Fru	1911.1, 307.1/307.1[j]	Baker[m]	quinic acid	QuiA	1889.5, 345.2	Sigma-Aldrich
fructose 6-phosphate	F6P	2352.1, 315	Fluka	raffinose	Raf	3492.6, 361.2	Sigma-Aldrich
fumaric acid	FumA	1349, 245.1	Sigma-Aldrich	rhamnose	Rha	1737, 117.1	Sigma-Aldrich
galacturonic acid	GalA	1977.4, 333.2	Sigma-Aldrich	D-ribose	D-Rib	1696.20, 307	Sigma-Aldrich
D-gluconic acid	D-GluA	2040.80, 292	Sigma-Aldrich	serine	Ser	1364.8, 204.2	Sigma-Aldrich
glucose	Gluc	1930.8, 205/217[j]	Baker	sorbitol	Sbt	1369.1, 319.2	Sigma-Aldrich
glucose-6-phosphate	G6P	2366, 387.2	Sigma-Aldrich	succinic acid	SucA	1316.1, 319.2	Sigma-Aldrich
glucuronic acid	GlucA	1973.9, 333	Sigma-Aldrich	sucrose	Suc	2702.9, 361	Sigma-Aldrich
glutamic acid	GluA	1624.8, 246.2	Pierce	threonic acid	ThrA	1393.7, 218	Fluka
glyceric acid	GlyA	1336, 147	Sigma-Aldrich	threonine	Thr	1393.7, 218	Sigma-Aldrich
glycerol	GlyOl	1279.8, 218	Sigma-Aldrich	L-valine	Val	1221.7, 144.2	Sigma-Aldrich
glycerol 3-phosphate	G3P	1775.9, 299.1	Sigma-Aldrich	xylitol	Xyl	1741.8, 307.2	Sigma-Aldrich
glycine	Gly	1308.7, 174.2	Fisher[n]	D-xylose	D-Xyl	1674.0, 217.1	Mann Research[o]

(C) Ace/MeOH; HPLC-MS			
metabolite	abbrev	mass spectral tag (corrected retention time, target ion)	coelution standard source
2,6,10-trimethyldodeca-2,7(*E*),9(*E*),11-tetra-6-ol	CTol[p]	3.85, 203	purified/identified
β-carotene	B-Car	20.02, 537	Fluka[q]
sitosteryl (6′-*O*-linolenoyl) *β*-D-glucoside	ASG1	20.608, 397	synthesized[r]
β-sitosterol	B-sito	17.75, 411	ChromaDex[s]
sitosteryl (6′-*O*-linoleoyl) *β*-D-glucoside	B-SGL	21.14, 397	synthesized[r]
sitosteryl (6′-*O*-stearate) *β*-D-glucoside	B-SGS	22.63, 397	synthesized[r]
β-sitosteryl linolenate	B-SL245	26.73, 397	synthesized[r]
β-sitosteryl linoleate	B-SL250	27.12, 397	synthesized[r]
β-sitosteryl palmitate	B-SP254	28.94, 397	synthesized[r]
campesteryl (6′-*O*-linolenoyl) *β*-D-glucoside	CGL	20.97, 383	synthesized[r]
chlorophyll *a*	ChlA	18.49, 893	Sigma-Aldrich[t]
chlorophyll *b*	ChLB	17.029, 893	Sigma-Aldrich
lutein	Lut	12.77, 551	Sigma-Aldrich
neoxanthin	NeXa	9.47, 583	ChromaDex
pheophytin	PheP	20.23, 871	synthesized[v]
ursolic/oleanic acid	UrsA	8.55, 439	Sigma-Aldrich
violaxanthin	VioX	9.99, 601	DHI Lab Products[u]

[a]Metabolites identified by authentic standards are listed according to extraction procedure, along with corresponding abbreviation used in figures, and mass spectral tag. [b]Sigma-Aldrich Co. LLC, St. Louis, MO, USA. [c]Purification and identification were performed as described in Rudell et al.[13] [d]J. T. Baker, Hayward, CA, USA. [e]Synthesis and purification were performed similar to the method of Fischer et al.[14] [f]Alfa Aesar, Ward Hill, MA, USA. [g]Fisher Scientific, Waltham, MA, USA. [h]Mallinckrodt Baker, Phillipsburg, NJ, USA. [i]TCI, Portland, OR, USA. [j]Results from two peaks pooled. [k]Sigma-Aldrich Co. LLC, St. Louis, MO, USA. [l]Fluka Chemical Co., Milwaukee, WI, USA. [m]J. T. Baker, Hayward, CA USA. [n]Fisher Scientific, Waltham, MA, USA. [o]Mann Research Center, Port St. Lucie, FL, USA. [p]Purification and identification were performed as described in Rudell et al.[13] [q]Fluka Chemical Co., Milwaukee, WI, USA. [r]Synthesized as described by Rudell et al.[7] [s]ChromaDex, Inc., Irvine, CA, USA. [t]Sigma-Aldrich Co. LLC, St. Louis, MO, USA. [u]DHI Lab Products, Hoersholm, Denmark. [v]10 mL of 0.05 mg mL^{-1} chl *a* + 10 drops 1 M HCl partitioned into diethyl ether.

(MSTs) were cataloged using the RI (or corrected retention time, LC-MS) coupled with the target ion used for semiquantitation and calibration tables generated using Chemstation (G1701DA rev. D; Agilent, Palo Alto, CA, USA). The Qedit macro was used to screen each peak and provide areas for semiquantitation. Mass spectral comparison with spectra cataloged in NIST05 (National Institute of Standards) and mass spectral interpretation aided in tentative identification of many of the components. Compound identifications were based on coelution and comparison of sample compound spectra and retention indices with those of authentic standards. Reference samples were run daily with GC-MS and LC-MS sequences to monitor the stability of the analytical systems. The reference sample consisted of a bulk sample of 'Granny Smith' peel. Levels of compounds were compared from GC-MS and LC-MS sequences from day to day; if levels drifted beyond ~10 relative standard deviations among the reference samples within a sequence or among the reference samples throughout the experiment, samples from that sequence were redone.

Chemicals. Metabolites identified by peak coelution with standards are listed in Table 1. Chemical standards were either purchased or obtained by a combination of synthesis and purification methods. (*E*,*E*)-*α*-Farnesene, (*Z*,*E*)-*α*-farnesene, 2,6,10-trimethyldodeca-2,7(*E*),9 (*E*),11-tetra-6-ol were purified and identified as previously described.[13] The Fischer esterification procedure[14] was performed to prepare 2-methylbutyl hexanoate, methyl 2-methylpropanoate, butyl hexanoate, butyl propanoate, ethyl pentanoate, and hexyl pentanaote. Briefly, 5 g of the organic acid and an excess of the alcohol (at least 2 times the molar equivalent of the organic acid) were refluxed for 1 h with 3 mL of concentrated sulfuric acid at the boiling point of the alcohol. The resulting mixture was then partitioned against 50 mL of water three times to remove the sulfuric acid and excess alcohol. Finally, the ester was redistilled to purify the final product; final purity was qualitatively assessed by GC-MS injection. Sitosteryl (6′-*O*-linolenoyl) *β*-D-glucoside, sitosteryl (6′-*O*-linoleoyl) *β*-D-glucoside, sitosteryl (6′-*O*-stearate), *β*-D-glucoside, *β*-sitosteryl linolenate, *β*-sitosteryl linoleate, *β*-sitosteryl palmitate, and campesteryl (6′-*O*-linoleoyl) *β*-D-glucoside were synthesized as previously described.[7]

Statistical Analysis. Data were analyzed to characterize metabolomic changes during cold storage and poststorage shelf life

while contrasting the effects of antioxidant treatment against the control group. Multivariate analyses were performed utilizing both supervised and unsupervised strategies. Supervised data analysis was performed to establish quantitative relationships between the *Y* matrix of experimental conditions and superficial scald response to the *X* matrix of metabolite levels using Unscrambler X 10.1 (Camo Software Inc., Woodbridge, NJ, USA). Partial least-squares (PLS) analysis was performed on metabolite concentrations separately for control and antioxidant-treated fruit peel. The data set was comprehensive, including metabolites identified by comparison to authentic standards as well as metabolites annotated according to mass spectral features and retention index (GC analyses) or retention time (LC analyses). Prior to PLS analysis, data were mean-centered and standard deviation scaled. Both models were subject to segmented cross-validation, with six segments each containing one sample from each treatment at each sampling point. Plots in Unscrambler were examined for outliers that were down-weighted in the final model. Variable's importance in projection (VIP) scores[15] were determined for each of the experimental factors.

Unsupervised multivariate analysis was performed using MetaboAnalyst.[16] Cluster analysis and heatmap generation were performed only for metabolites with identification confirmed by coelution with authentic standards. Prior to analysis using MetaboAnalyst, data were averaged across sample replicates, mean-centered, and divided by the square root of the standard deviation of each metabolite (autoscaling). Ward's clustering algorithm and Pearson's distance were used for cluster analysis. Heatmaps were used to depict cluster analysis results, where the degree of relative response is represented by color using a gradient representing low to high response values. In the cluster analysis and heatmap, treatment groups were ordered according to increasing storage duration, effectively limiting cluster analysis to similarities in metabolite response.

To determine the metabolites associated with superficial scald, two-way analysis of variance (ANOVA) was performed using MetaboAnalyst with Bonfferoni's correction procedure used to control level of significance (p) error rate.

RESULTS

Superficial Scald Development. Scald severity, assessed immediately upon removal from cold temperature, was apparent at 120 days and increased between 120 and 180 days as well as during the 14 days of shelf life at 20 °C following cold storage for both time points (Figure 1). DPA treatment inhibited scald development.

Metabolites Profiled from 'Granny Smith' Apple Peel. Over 800 unique metabolic signatures from apple peel tissue were detected by the use of several extraction methods; a subset was further identified by peak coelution with authentic standards (listed in Table 1). Metabolites not listed were annotated according to a mass spectral tag consisting of a retention index or retention time and mass spectrum.

Effects of Antioxidant Treatment, Storage, Shelf Life, and Superficial Scald Development on the Metabolic Profile of 'Granny Smith' Apple Peel. Five factors (PLS components) captured >90% of the variance for calibration and prediction in the PLS model for control fruit, indicating that the majority of the variance is accounted for by the first few factors of the model. For control fruit, the PLS scores plot (Figure 2A) and loadings plot (Figure 2B) result from the same PLS modeling procedure, but illustrate different aspects of the peel metabolome. The effects of storage duration and superficial scald on overall metabolism of control fruit peel are shown in the scores plot (Figure 2A). The close proximity of the data points in Figure 2A (representing sampling dates) indicates similarities in metabolomics trends: early shelf life periods (following harvest and 30 days of cold storage) are relatively

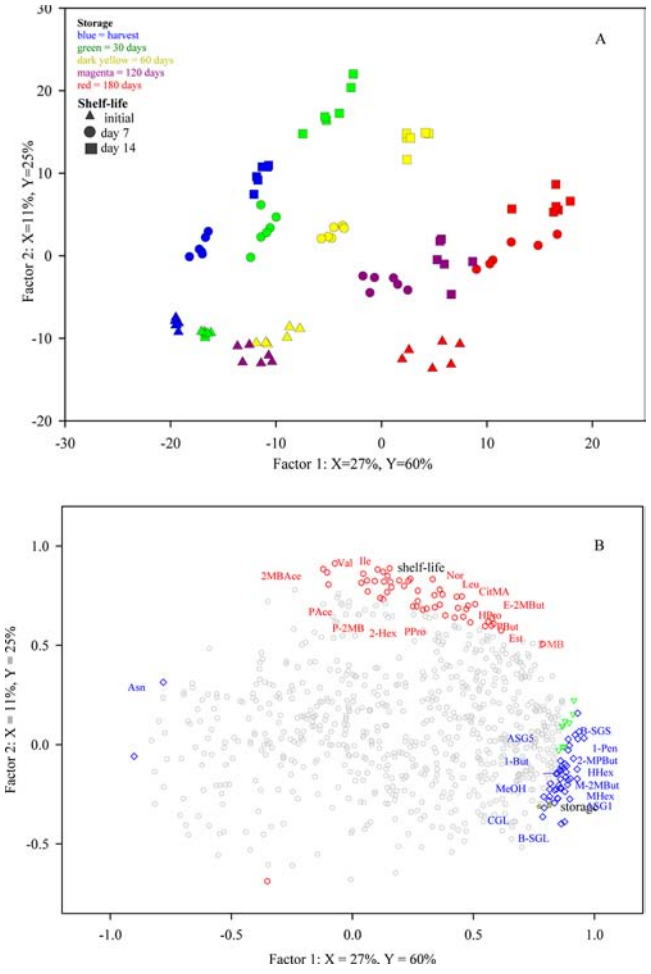

Figure 2. (A) PLS analysis scores plot incorporating storage duration and shelf life changes in control fruit. Storage duration and shelf life duration for each observation are indicated by label. Storage (at 1 °C): at harvest initial sample (blue); 30 days (green); 60 days (dark yellow); 120 days (magenta); and 180 days (red). Shelf life at 20 °C: immediate sampling (triangles), 7 days (circles), and 14 days (squares). (B) PLS loadings plot incorporating storage duration and shelf life changes in control fruit. Metabolites identified by authentic standards are listed by abbreviation; metabolites identified primarily by mass spectral features (MST) are represented by a dot. Metabolites with high VIP scores for shelf life are indicated in red; storage and scald are indicated in blue.

similar, while increasing length of cold storage prior to shelf life (60, 120, and 180 days of cold storage) results in an increasingly disparate metabolome. The loadings plot (Figure 2B) indicates metabolites associated with storage duration, shelf life, and superficial scald by their proximity to each of these experimental factors. Mathematically, this proximity is determined by the VIP score, which is a measure of how closely the metabolites are associated with either storage, shelf life, or superficial scald. Metabolites or mass spectral tages within the top 50 VIP scores for storage, shelf life, or superficial scald are indicated in the plots. The PLS analysis of DPA-treated fruit can be interpreted in a similar manner (Figure 3). PLS analysis of changes in the antioxidant-treated peel metabolome was represented in four factors (>90% for both the calibration and prediction variance). Again, for DPA-treated fruit, PLS scores (Figure 3A) and loadings (Figure 3B) result from the same data analysis procedure. Differential effects of

dx.doi.org/10.1021/jf3046208 | J. Agric. Food Chem. 2013, 61, 1373−1387

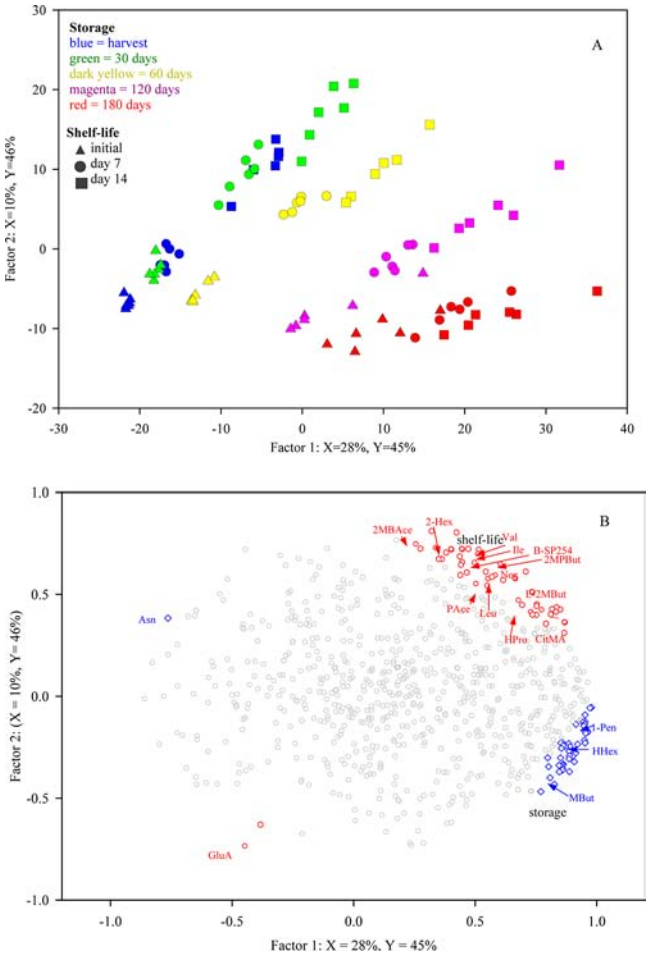

Figure 3. (A) PLS analysis scores plot incorporating storage duration and shelf life changes in DPA-treated fruit. Storage and shelf life for each observation are indicated by label. Storage (at 1 °C): at harvest initial sample (blue); 30 days (green); 60 days (dark yellow); 120 days (magenta); and 180 days (red). Shelf life at 20 °C: immediate sampling (triangles), 7 days (circles), and 14 days (squares). (B) PLS analysis loadings plot incorporating storage duration and shelf life changes in DPA-treated fruit. Identified metabolites are listed by abbreviation; unidentified metabolites are represented by a dot. Metabolites with high VIP scores for shelf life are indicated in red and storage in dark yellow.

storage duration and shelf life of DPA-treated fruit on overall metabolism are illustrated in the scores plots (Figure 3A). Overall, shelf life trends between control and DPA-treated fruit appear to be similar: like control fruit, the DPA-treated fruit had greater similarity among samples during early storage and shelf life periods (following harvest and 30 days of cold storage), whereas increasing cold storage prior to ambient-temperature shelf life resulted in an increasingly different metabolome. Metabolites associated with storage duration and shelf life in DPA-treated fruit peel are apparent in the loadings plots (Figure 3B). Some metabolites associated with shelf life and storage were common to both treatments, whereas others differed. VIP values ranged from 0.71 to 0.92. Metabolites highly associated with the shelf life using the VIP procedure, irrespective of the storage duration or treatment, included ethyl 2-methylbutyrate, 2-methylbutyl acetate, pentyl acetate, hexyl propanoate, 2-hexenal, 2-methylpropyl butyrate, leucine, isoleucine, norvaline, valine, and citramalic acid. In the PLS model of control fruit, the superficial scald and storage were closely linked. Metabolites highly associated with these variables according to the VIP procedure included 1-pentanol, 1-butanol, hexyl hexanoate, methyl 2-methyl butyrate, methyl hexanoate, methanol, sitosteryl (6′-*O*-stearate) *β*-D-glucoside, sitosteryl (6′-*O*-linoleoyl) *β*-D-glucoside, sitosteryl (6′-*O*-linolenoyl) *β*-D-glucoside, and campesteryl (6′-*O*-linolenoyl) *β*-D-glucoside. In contrast, metabolites highly associated with storage in the PLS model of DPA fruit peel according to the VIP procedure included 1-pentanol, hexyl hexanoate, and methyl butyrate.

Cluster analysis revealed cofluctuation of metabolite levels during cold storage and poststorage ripening, as well as in response to DPA treatment (Figure 4; Table 2). The cluster features most clearly differentiated by treatment included acetone, 2-butanol, CTol, MHO, 6-methyl-5-hepten-2-ol (MHol), campesteryl (6′-*O*-linolenoyl) *β*-D-glucoside, sitosteryl (6′-*O*-linoleoyl) *β*-D-glucoside, and sitosteryl (6′-*O*-linolenoyl) *β*-D-glucoside (in cluster A) and inositol, methanol, methyl acetate, methyl propanoate, methyl hexanoate, methyl butyrate, methyl 2-methylbutyrate, methyl 2-methyl propanoate, glucuronic acid, gluconic acid, pipecolic acid, ribose, and sitosteryl (6′-*O*-stearate) *β*-D-glucoside (in cluster B). An additional cluster differentiated by treatment, with levels generally higher in control fruit, included galacturonic acid, mucic acid, and xylose. Pigments, including *β*-carotene, violaxanthin, chlorophylls *a* and *b*, as well as malic acid, decreased overall during shelf life at harvest and following 30 days of cold storage, but levels remained higher in DPA-treated fruit. Metabolite levels that decreased during storage, regardless of antioxidant treatment, were a heterogeneous group of primary metabolites consisting of proline, pyruvic acid, maleic acid, fructose-6-phosphate, 2-oxoglutaric acid, phenylalanine, and *γ*-aminobutyric acid (GABA). An additional cluster contained metabolites that were generally more abundant immediately following removal from cold storage at 120 days for both treatments. Metabolites in this cluster included glucose, sorbitol, (*E*,*E*)-*α*-farnesene, (*Z*,*E*)-*α*-farnesene, *β*-farnesene, ursolic acid, and raffinose. Cofluctuations during shelf life included the amino acids valine, norvaline, leucine, and isoleucine, for which the highest responses are apparent at the final day of shelf life following 30, 60, and 120 days of storage. Additional areas of coordinated control included volatile esters containing similar moieties throughout shelf life periods. These include methyl, ethyl, propyl/propanoate, butyl/butyrate, acetate, and hexyl/hexanoate moieties. Aroma volatile levels also differed according to storage duration prior to shelf life: acetate esters peaked early in storage; ethyl, propyl, and propanoate esters peaked midstorage; methyl, butyl/butanoate, and hexyl/hexanoate esters peaked later in storage.

Metabolite levels differed significantly between control and DPA-treated fruit peel (Table 3), and the impact of DPA treatment was almost immediately apparent. The contents of several volatile compounds and the flavanols epicatechin and catechin remained high or were significantly higher in control fruit, whereas levels dropped in DPA-treated fruit within the time following DPA application and peel sampling at harvest. *α*-Farnesene content was higher in DPA-treated fruit compared with control fruit at both 60 and 120 days; levels of *α*-farnesene oxidation products, including MHO and MHol content, were higher in control fruit as early as 30 days into storage, well before scald symptoms were apparent at 120 days. Levels of sitosteryl (6′-*O*-linolenoyl) *β*-D-glucoside, sitosteryl (6′-*O*-linoleoyl) *β*-D-glucoside, and campesteryl (6′-*O*-linolenoyl) *β*-

dx.doi.org/10.1021/jf3046208 | *J. Agric. Food Chem.* 2013, 61, 1373−1387

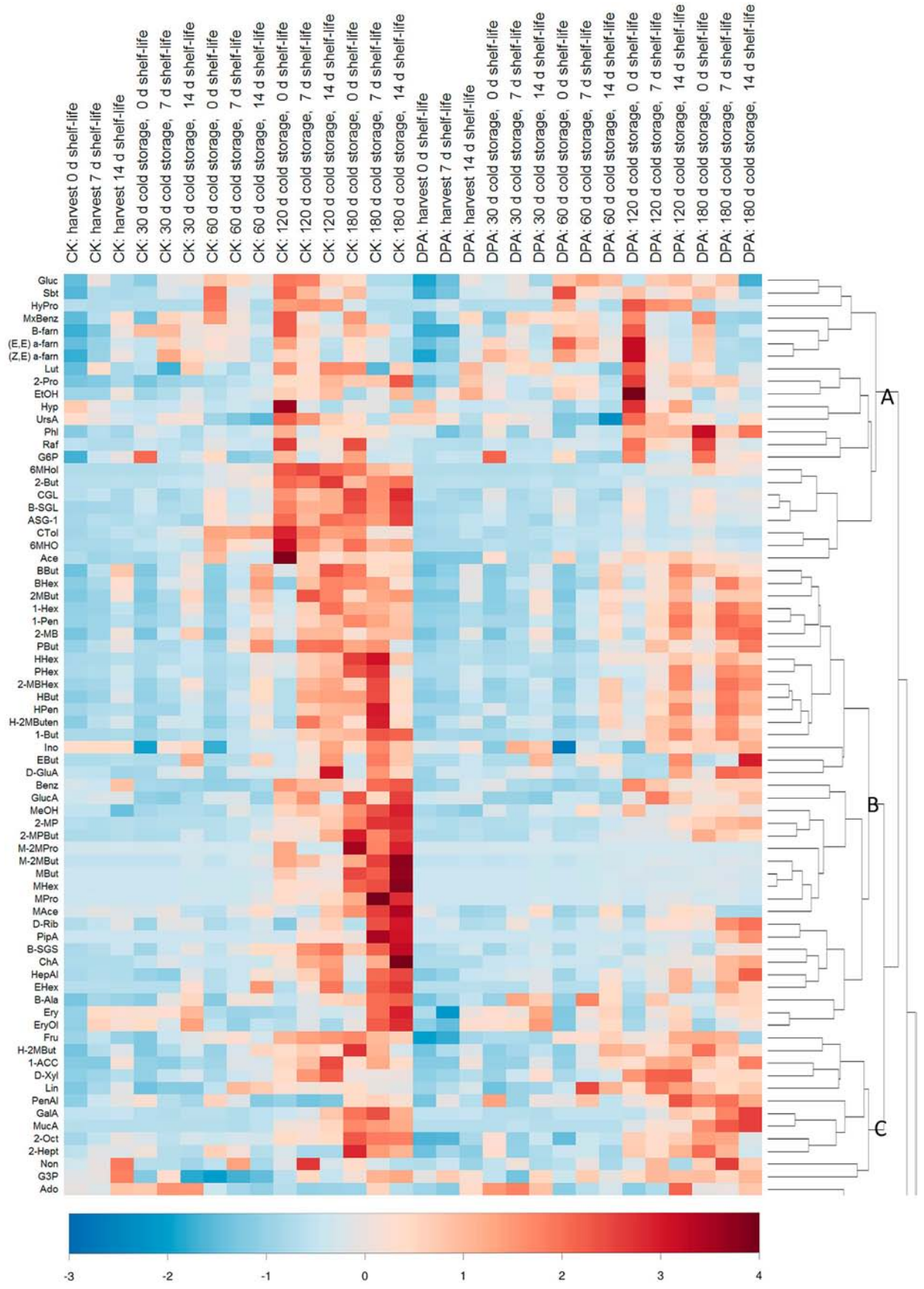

Figure 4. continued

dx.doi.org/10.1021/jf3046208 | *J. Agric. Food Chem.* 2013, 61, 1373−1387

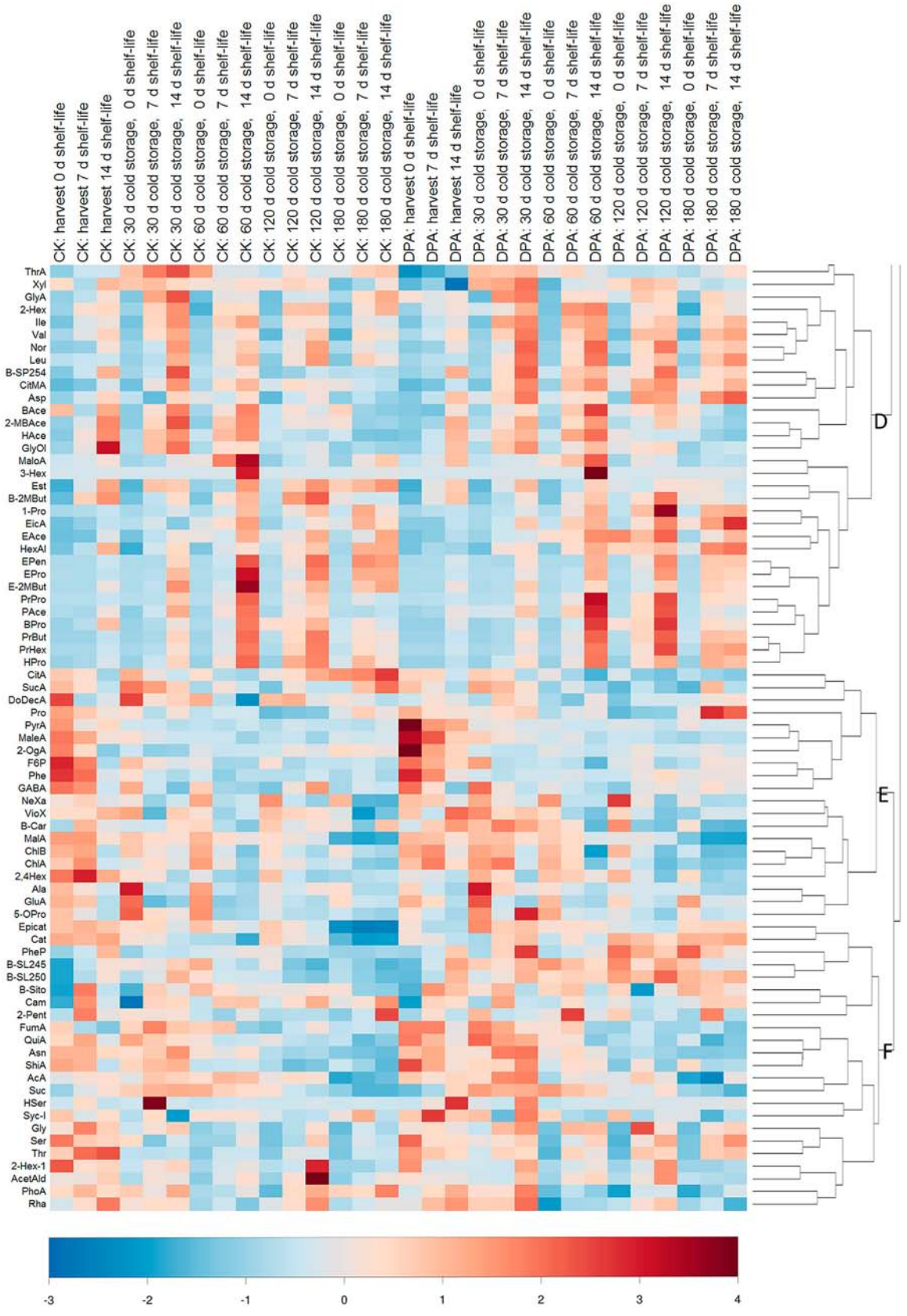

Figure 4. Heatmap illustrating cluster analysis using Ward's clustering algorithm and Euclidean distance grouped metabolites according to similarities in fluctuations as affected by cold storage duration, shelf life duration, and antioxidant treatment. Data were mean-centered and divided by the square root of the stand deviation of each metabolite prior cluster analysis. The color gradient indicates low to high relative levels of metabolites. Higher order clusters are indicated by letters A–I, and metabolites in each lettered cluster are indicated in Table 2.

dx.doi.org/10.1021/jf3046208 | J. Agric. Food Chem. 2013, 61, 1373–1387

Table 2. Cluster Analysis Using Ward's Clustering Algorithm and Pearsons's Distance Grouped Metabolites According to Similarities in Metabolite Fluctuations As Affected by Cold Storage Duration, Shelf Life Duration, and Antioxidant Treatment[a]

A	B	C	D	E	F
sorbitol	butyl butyrate	fructose	adonitol	citramalic acid	epicatechin
hyroxyproline	butyl hexanoate	hexyl 2-methylbutyrate	threonic acid	succinic acid	catechin
methoxybenzene	2-methylbutyrate	1-aminocyclopropane-1-carboxylic acid	xylose	dodecanoic acid	pheophytin
β-farnesene	1-hexanal	D-xylose	glyceric acid	proline	β-sitosteryl linolenate
(*E*,*E*)-α-farnesene	1-pentanal	linoleic acid	2-hexenal	pyruvic acid	β-sitosteryl linoleate
(*Z*,*E*)-α-farnesene	2-methylbutanol	pentanal	isoleucine	maleic acid	β-sitosterol campesteryl
lutein	pentyl butyrate	galacturonic acid	valine	2-oxoglutaric acid	(6′-*O*-linolenoyl) β-D-glucoside
2-propanol	hexyl hexanoate	mucic acid	norvaline	fructose-6-phosphate	(*E*)-2-pentenal
ethanol	pentyl hexanoate	2-octenal	leucine	phenylalanine	fumaric acid
hyperin	2-methylbutylhexanoate	2-heptanal	β-sitosteryl palmitate	γ-aminobutyric acid	quinic acid
ursolic acid	hexyl butyrate	nonanal	citramalic acid	neaxanthin	asparagine
phloridzin	hexyl pentanoate	glucose-3-phosphate	L-aspartic acid	violaxanthin	shikimic acid
raffinose	hexyl 2-methylbutenoate		butyl acetate	β-carotene	acetic acid
glucose-6-phosphate	1-butanol		2-methylbutyl acetate	malic acid	sucrose
6-methyl-5-hepten-2-ol	inositol		hexyl acetate	chlorophyll *a*	*scyllo*-inositol
2-butanol	ethyl butyrate		glycerol	chlorophyll *b*	threonine
campesteryl (6′-*O*-linolenoyl) β-D-glucoside	D-gluconic acid		malonic acid	(*E*,*E*)-2,4-hexadienal	(*Z*)-2-hexen-1-ol
sitosteryl (6′-*O*-linoleoyl) β-D-glucoside	benzaldehyde		3-hexenal	alanine	acetaldehyde
sitosteryl (6′-*O*-linolenoyl) β-D-glucoside	glucuronic acid		estragole	glutamic acid	phosphoric acid
2, 6, 10-trimethyldodeca-2,7(*E*),9(*E*),11-tetra-6-ol	methanol		butyl 2-methyl-butyrate	5-oxoproline	rhamnose
6-methyl-5-hepten-2-one	2-methyl-1-propanol		1-propanol		
acetone	2-methylpropylbutyrate		eicosanoic acid		
	methyl 2-methylpropanoate		ethyl acetate		
	methyl 2-methylbutyrate		hexanal		
	methyl butyrate		ethyl pentanoate		
	methyl hexanoate		ethyl propanoate		
	methyl propanoate		ethyl 2-methyl-butyrate		
	methyl acetate		propyl propanoate		
	D-ribose		propyl acetate		
	pipecolic acid		propyl butyrate		
	sitosteryl (6′-*O*-stearate) β-D-glucoside		propyl hexanoate		
	chlorogenic acid		hexyl propanoate		
	heptanal				
	ethyl hexanoate				
	β-alanine				
	erythrose				
	erythritol				

[a]For discussion purposes, higher order clusters are indicated in Figure 4; metabolites are listed here corresponding to each cluster.

D-glucoside were elevated in control fruit, also prior to symptom development. At 30 days, in addition to volatile compounds, 2-oxoglutaric acid, pheophytin, β-alanine, and quinic acid differed significantly between treatments. By 60 days, the list of significantly differing compounds also included (*Z*,*E*)- and (*E*,*E*)-α-farnesene, 2-butanol, several methyl and ethyl esters, various phytosterol compounds, pheophytin, glycine, and valine. At 120 and 180 days, when scald symptoms were present, differentiating metabolites included many of the compounds that were different at earlier time points. Compounds that differed at 120 and 180 days still included phenylpropanoid-derived compounds (chlorogenic acid at 120 days and epicatechin/catechin at 180 days), methyl esters, pheophytin, aspartic acid, glutamic acid, serine, and erythritol, inositol, and sorbitol, whereas ethyl ester and hexyl ester contents were different at 120 and 180 days, respectively.

DISCUSSION

Antioxidant Treatment Affects Metabolic Processes Associated with Chilling Injury. The prevention of superficial scald by DPA has been attributed to its antioxidant

Table 3. Significant Differences in Metabolite Response Levels As Affected by Treatment and Shelf Life Duration Determined Individually at Harvest and at 30, 60, 120, and 180 Days of Cold Strorage by Two-Way ANOVA with One Factor as Time during Post-Cold-Storage Shelf Life[a]

metabolite	treatment	higher levels	shelf life	control shelf life trend	DPA shelf life trend	interaction
			Harvest			
(*E*,*E*)-2,4-hexadienal	***	CK	***	incr/decr	no change	*
(*Z*)-2-hexen-1-ol	**	CK	***	decrease	decrease	ns
butyl 2-methylbutyrate	***	CK	***	increase	increase	***
catechin	***	CK	ns	no change	decrease	ns
epicatechin	**	CK	*	no change	decrease	*
hexyl acetate	**	CK	***	increase	increase	ns
nonanal	**	CK	**	increase	no change	***
threonic acid	***	CK	**	increase	increase	ns
			30 Days of Storage			
2,6,10-trimethyldodeca-2,7(*E*),9(*E*),11-tetra-6-ol	***	CK	***	increase	increase	**
2-methylbutanol	*	CK	***	increase	increase	ns
2-oxoglutaric acid	*	DPA	ns	no change	no change	ns
2-propanol	*	DPA	ns	no change	no change	ns
6-methyl-5-hepten-2-ol	*	CK	***	increase	increase	*
6-methyl-5-hepten-2-one	***	CK	ns	no change	no change	*
β-alanine	*	DPA	***	increase	incr/decr	ns
butyl acetate	*	CK	***	increase	increase	ns
ethyl hexanoate	*	CK	***	increase	increase	***
ethyl propionate	**	CK	***	increase	increase	***
pheophytin	***	DPA	***	no change	increase	**
quinic acid	**	DPA	ns	no change	no change	ns
			60 Days of Storage			
2,6,10-trimethyldodeca-2,7(*E*),9(*E*),11-tetra-6-ol	***	CK	ns	no change	no change	ns
(*E*)-2-hexenal	*	DPA	***	increase	increase	ns
(*E*,*E*)-2,4-hexadienal	*	DPA	**	decrease	decrease	ns
(*E*,*E*)-α-farnesene	***	DPA	***	decrease	decrease	ns
(*Z*,*E*)-α-farnesene	*	DPA	**	decrease	decrease	ns
2-butanol	**	CK	ns	no change	no change	ns
ethyl 2-methylbutyrate	*	CK	***	increase	increase	***
6-methyl-5-hepten-2-ol	***	CK	ns	no change	no change	ns
6-methyl-5-hepten-2-one	***	CK	***	decrease	no change	***
sitosteryl (6′-*O*-linoleoyl) β-D-glucoside	*	CK	***	decrease	decrease	ns
sitosteryl (6′-*O*-stearate) β-D-glucoside	**	CK	***	increase	increase	***
campesteryl (6′-*O*-linolenoyl) β-D-glucoside	**	CK	***	decr/incr	decr/incr	ns
ethyl hexanoate	*	CK	***	increase	increase	***
ethyl pentanoate	**	CK	***	increase	increase	**
ethyl propionate	**	CK	***	increase	increase	***
glycine	***	DPA	***	increase	increase	*
methyl butyrate	**	CK	***	increase	increase	***
methyl propionate	**	CK	***	increase	increase	*
pentyl butyrate	**	CK	**	increase	increase	ns
valine	**	DPA	***	increase	increase	***
			120 Days of Storage			
2,6,10-trimethyldodeca-2,7(*E*),9(*E*),11-tetra-6-ol	***	CK	***	decrease	no change	***
1-propanol	**	DPA	***	increase	increase	**
2-methylpropanol	**	CK	***	increase	increase	ns
2-butanol	***	CK	ns	no change	no change	ns
(*Z*)-2-hexen-1-ol	**	CK	***	increase	increase	*
2-methylpropyl butyrate	**	CK	***	decr/incr	no change	**
(*E*,*E*)-α-farnesene	***	DPA	***	decrease	decrease	*
(*Z*,*E*)-α-farnesene	**	DPA	**	decrease	decrease	*
6-methyl-5-hepten-2-ol	***	CK	ns	no change	no change	ns
6-methyl-5-hepten-2-one	***	CK	***	decrease	no change	***
aspartic acid	**	DPA	***	increase	increase	*

Table 3. continued

metabolite	treatment	higher levels	shelf life	control shelf life trend	DPA shelf life trend	interaction
			120 Days of Storage			
acetaldehyde	*	CK	***	increase	increase	***
acetone	*	CK	***	decrease	no change	***
sitosteryl (6′-*O*-linoleoyl) β-D-glucoside	***	CK	***	decrease	decr/incr	ns
sitosteryl (6′-*O*-stearate) β-D-glucoside	***	CK	***	increase	increase	ns
β-sitosteryl linoleate	**	DPA	ns	no change	no change	ns
β-sitosteryl palmitate	***	DPA	***	increase	increase	ns
campesteryl (6′-*O*-linolenoyl) β-D-glucoside	***	CK	**	decr/incr	decr/incr	ns
chlorogenic acid	***	CK	**	increase	increase	ns
citramalic acid	**	DPA	***	incr/decr	increase	***
estragole	**	CK	***	increase	increase	***
ethyl 2-methylbutyrate	*	CK	***	increase	increase	*
ethyl hexanoate	***	CK	***	increase	increase	***
glutamic acid	***	DPA	***	decrease	decrease	ns
glycerol	**	DPA	*	increase	increase	ns
glycerol 3-phosphate	*	DPA	ns	no change	no change	ns
inositol	**	CK	***	increase	incr/decr	**
methyl 2-methylbutyrate	***	CK	ns	no change	no change	ns
methyl butyrate	***	CK	***	decrease	no change	***
methyl hexanoate	***	CK	ns	no change	no change	ns
methyl propionate	*	CK	ns	no change	no change	ns
methyoxybenzene	*	CK	***	decrease	decrease	ns
pentanal	*	DPA	ns	no change	no change	ns
pheophytin	***	DPA	ns	no change	no change	ns
phosphoric acid	**	CK	***	increase	increase	ns
propyl acetate	*	DPA	***	increase	increase	*
propyl propionate	**	DPA	***	increase	increase	***
serine	*	DPA	***	increase	increase	*
sorbitol	*	CK	***	decrease	decrease	***
succinic acid	**	CK	***	increase	increase	ns
valine	**	DPA	***	increase	increase	*
			180 Days of Storage			
2-butanol	*	CK	ns	increase	no change	ns
2-methylbutanol	**	DPA	***	increase	increase	*
2-methylpropanol	*	DPA	ns	increase	increase	ns
2-methylpropyl butyrate	***	CK	*	incr/decr	decrease	ns
5-oxoproline	**	DPA	***	decrease	no change	ns
6-methyl-5-hepten-2-ol	***	CK	***	decrease	decrease	ns
6-methyl-5-hepten-2-one	***	CK	***	decrease	decrease	**
ascorbic acid	***	DPA	ns	decrease	no change	ns
asparagine	**	DPA	ns	decrease	increase	ns
aspartic acid	***	DPA	ns	no change	increase	ns
benzaldehyde	**	CK	***	increase		*
sitosteryl (6′-*O*-linoleoyl) β-D-glucoside	***	CK	ns	no change	no change	ns
sitosteryl (6′-*O*-stearate) β-D-glucoside	***	CK	***	increase	no change	*
β-sitosteryl linoleate	***	DPA	ns	no change	no change	ns
campesteryl (6′-*O*-linolenoyl) β-D-glucoside	***	CK	**	decr/incr	no change	ns
catechin	***	DPA	ns	no change	no change	ns
citramalic acid	***	DPA	ns	decrease	increase	***
citric acid	***	CK	ns	increase	decrease	ns
D-xylose	**	DPA	ns	no change	no change	ns
epicatechin	***	DPA	ns	no change	no change	ns
erythritol	**	CK	ns	increase	increase	ns
estragole	***	CK	ns	increase	decrease	ns
hexyl acetate	**	DPA	***	decrease	decrease	*
hexyl hexanoate	***	CK	***	incr/decr	incr/decr	***
isoleucine	*	DPA	***	incr/decr	increase	***
leucine	*	DPA	***	incr/decr	increase	*
methyl 2-methylbutyrate	***	CK	***	increase	no change	***

dx.doi.org/10.1021/jf3046208 | J. Agric. Food Chem. 2013, 61, 1373−1387

Table 3. continued

metabolite	treatment	higher levels	shelf life	control shelf life trend	DPA shelf life trend	interaction
			180 Days of Storage			
methyl acetate	***	CK	ns	increase	decrease	**
methyl alchol	***	CK	ns	increase	no change	**
methyl butyrate	***	CK	***	increase	no change	***
methyl hexanoate	***	CK	**	increase	no change	***
methyl propionate	**	CK	ns	incr/decr	no change	ns
norvaline	*	DPA	***	incr/decr	increase	ns
pheophytin	***	DPA	**	no change	decrease	***
phosphoric acid	***	CK	ns	no change	increase	ns
pipecolic acid	***	CK	***	incr/decr	increase	**
propyl propionate	*	DPA	***	incr/decr	incr/decr	ns
serine	**	DPA	***	incr/decr	increase	***
valine	***	CK	***	incr/decr	increase	ns

[a] $p < 0.05$, *; $p < 0.01$,**; $p < 0.001$, ***. Multiple-test correction procedure used was Bonferroni's. Only metabolites with significant differences according to treatment are shown.

capacity,[1,6,17] which ameliorates oxidative stress associated with the chilling injury that leads to superficial scald development.[17] In addition, the metabolic differences between treatments observed in this study indicate DPA has broad impacts on fruit metabolism beyond mechanisms responsible for ameliorating superficial scald; metabolome-wide divergence due to DPA treatment been documented.[17]

Oxidation products of α-farnesene, including CTol, MHO, and MHol, have been linked with scald in multiple studies.[2,18,19] Whether they are directly responsible for superficial scald symptoms or are a byproduct of the oxidative processes that are assumed to lead to cell death is still unclear,[1] although metabolites resulting from α-farnesene oxidation exceed a certain threshold before symptoms are observed,[20] and application of α-farnesene oxidation products can provoke scald-like symptoms.[21]

Elevated levels of acylated steryl glucosides and steryl esters may reflect changes in cell membrane integrity and functionality.[22] Increased sterol conjugation in peel tissue alongside scald development has been reported where the transition of fruit from cold storage to shelf life temperatures is also accompanied by a shift from unsaturated to saturated fatty acyl moieties of acylated steryl glycosides and steryl esters.[7] Elevated inositol levels early in storage could also indicate changes in cell membranes; among many other possible roles in cell metabolism, it can be a component of structural lipids.[23] These metabolic changes may indicate modifications in the plasma membrane due to chilling injury or oxidative stress. Corroborating these results, previous work indicates DPA effects include preservation of cell membrane integrity during long-term cold storage.[24]

Corresponding increases of methyl esters with pectic acids and superficial scald development in both cold storage and shelf life conditions indicate changes in cell wall structure differentiated by treatment. It has been demonstrated that DPA treatment affects fruit senescence or ripening pathways, including cell wall disassembly.[25] The degree of pectin polymerization in the middle lamella decreases in senescent apple fruit,[26] which corresponds with increases of free pectic acid residues. Although the cell wall disassembly that takes place during ripening is catalyzed by polysaccharide-modifying enzymes,[24] hydroxyl radicals can cause nonenzymatic scission of polysaccharides,[27] suggesting a role for antioxidant protection in the retention of cellular integrity. The degree of pectin methyl esterification decreases during cell wall disassembly.[28] Pectin methyl esterase activity catalyzes the production of methanol in tomato fruit.[29] Apples supplied with primary alcohols exhibit increased production of ester containing the feed alcohol moiety,[30] and it is generally accepted that substrate availability, rather than enzyme activity, limits apple volatile production.[31,32] Elevated levels of all of these compounds in scalded fruit suggest cell wall disassembly is occurring simultaneously and that released methanol is combined with various acyl moieties to form methyl esters.

Chloroplastic pigments were also altered by DPA treatment. Reduced chlorophyll fluorescence occurs prior to superficial scald development,[33] and chlorophyll excitation is used commercially as a measure of storage stress in apple fruit,[34] yet the existence or nature of any relationship between superficial scald and changes in the photosystem represented by recovery of these pigments is not well characterized. During ripening, due to chlorophyll degradation and partial retention of carotenoids,[35] increasing levels of carotenoids and decreased chlorophyll *a* and *b* content have been observed[36,37] contributing to peel color changes[38] and photoprotection in senescing tissues.[37] Pheophytin can be an intermediate electron acceptor in photosystem II[39] or a degradative product of chlorophyll provoked by heat or reduced pH.[40] Chlorophyll catabolism is a complex process tightly regulated during plant senescence;[35,41] plants lacking key chlorophyll degradation enzymes may exhibit lesion and cell death phenotypes.[41] Superficial scald symptoms have similarities to lesions characteristic of the hypersensitive response, and it has previously been suggested that the browning reaction associated with superficial scald is caused by polyphenol oxidase released from chloroplasts.[5] Different patterns of decrease of photoreactive pigment levels between treatments and decreased pheophytin levels in the control fruit may be related to differential chlorophyll degradation and superficial scald development. Importantly, these events precede scald symptom induction, although differential photosystem disassembly cannot be definitively implicated in scald development by this study.

Combined Effects of Storage and Shelf Life Conditions Reveal Coregulation of Volatile Ester Synthesis. Transition of apples to warm temperatures after cold storage is

generally characterized by physiological changes that are considered hallmarks of apple fruit ripening. During ripening, ethylene production and respiration increase, primary cell walls and membranes are modified,[24] and overall volatile production increases.[42] Cold storage duration had a marked effect on the metabolome, but several groups of metabolites exhibited relatively constant levels of response during shelf life irrespective of cold storage preceding warmer shelf life conditions. The consistent link of branched-chain amino acids to shelf life conditions may result from increased fruit metabolic activity at warmer temperatures, as they are ultimately derived from the tricarboxylic acid cycle.[43] Valine and isoleucine can be substrates for 2-methylpropyl and 2-methylbutyl moieties of volatile esters.[44,45] Elevated levels of citramalate alongside isoleucine support an alternate biosynthetic pathway for this amino acid postulated by Sugimoto et al.[45] Importantly, pentyl acetate and ethyl 2-methylbutyrate are among the compounds with the highest sensorial impact for 'Granny Smith' apples.[46] Their reliable response to shelf life conditions irrespective of treatment or storage duration prior to shelf life indicates consistent substrate and process availability and activity related to their biosynthesis.

The relative change in abundance of volatile esters containing a particular moiety responding to temperature and chemical treatment supports the increasingly nuanced view of volatile biosynthesis that incorporates evidence of changes in gene expression for enzymes involved in both substrate production and penultimate biosynthesis[47] rather than primarily constitutive expression of enzymes catalyzing the final steps of this process. Volatile ester synthesis is influenced by many factors, including ethylene-regulated ripening processes, although only some aspects of biosynthesis are under strict ethylene control. Multiple enzymes contribute to volatile ester biosynthesis. Precursors of volatile esters can be produced in the lipoxygenase (LOX) pathway and by β-oxidation of fatty acids.[48] LOX activity has been associated with tissue disruption, ripeness and aging.[49] The final step of ester biosynthesis is the condensation of the alcohol and activated (coenzyme A) carboxylic acid moieties catalyzed by alcohol acyltransferases (AAT).[50] The activity of alcohol dehydrogenases (ADH) often precedes this step by the reversible reduction of aldehydes to alcohols. Although exogenous feeding of alcohols or acids to fruit disks indicates that these compounds can act as precursors to limit or increase production of esters containing corresponding moieties,[31,48] ADH and AAT may have substrate specificity, be localized in different tissues, and exhibit diverse expression levels during ripening.[51] ADH transcription increases at 20 °C, yet activity is regulated by post-transcriptional mechanisms. AATs may be constitutively expressed.[47]

Tracking levels of esters grouped by moiety illustrates that the metabolic processes related to ripening and senescence generate differing substrates for ester biosynthesis as fruit ages in storage. Substrate for acetate esters, which peaked early in storage, may be generated from glycolysis or β-oxidation products of fatty acids.[31] Ethyl ester production, which exhibited highest levels midstorage, is likely associated with ethanol availability, often attributed to anaerobic respiration;[31] specifically, the activity of pyruvate decarboxylase (PDC) and ADH on pyruvate derived from the glycolytic pathway as well as from stress responses.[50,52] Later in storage, butyl/butanoate and hexyl/hexanoate esters may reflect increasing LOX activity and β-oxidation of C6 fatty acid LOX products.[53] As expected, contrasting control fruits, which developed scald, with DPA-treated fruits, which were asymptomatic, enabled identification of metabolites uniquely associated with disorder development. It was expected that superficial scald development in control fruit, contrasted with asymptomatic fruit treated with DPA, would enable identification of metabolites uniquely associated with disorder development. In addition, the untargeted nature of metabolomic evaluation coupled with appropriate statistical analyses enabled further discovery of metabolic trends, such as the described coordination among volatile esters linked to underlying trends in available substrate related to fruit aging.

The results of this study indicate differential cell wall disassembly, methyl ester production, and chlorophyll catabolism may occur in control fruits, which develop superficial scald peel injury, compared to DPA-treated fruits, which remain asymptomatic. In addition, coordinated changes according to moieties in volatile ester production indicate a combination of dynamic substrate genesis, volatile ester pathway plasticity, and possibly changing genetic regulation responding to temperature conditions and cold-storage duration. These results lend insight into metabolic processes related to superficial scald, chilling injury, and oxidative stress, as well as demonstrate the utility of metabolomics for revealing novel aspects of physiology related to disorder development, storage longevity, and consumer appeal in food crops.

AUTHOR INFORMATION

Corresponding Author

*Phone: 1 (509) 664-2280, ext. 245. E-mail: David.Rudell@ars.usda.gov.

Notes

The authors declare no competing financial interest.

ACKNOWLEDGMENTS

We gratefully acknowledge the assistance of Chris Sater, Brad Wright, and Nate Sullivan with figure preparation and sample processing.

ABBREVIATIONS USED

DPA, diphenylamine; CTol, 2,6,10-trimethyldodeca-2,7(*E*),9-(*E*),11-tetra-6-ol; MHO, 6-methyl-5-hepten-2-one; MHol, 6-methyl-5-hepten-2-ol; VIP, variable importance in projection

REFERENCES

(1) Lurie, S.; Watkins, C. B. Superficial scald, its etiology and control. *Postharvest Biol. Technol.* **2012**, *65*, 44−60.

(2) Whitaker, B. D.; Saftner, R. A. Temperature-dependent autoxidation of conjugated trienols from apple peel yields 6-methyl-5-hepten-2-one, a volatile implicated in the induction of scald. *J. Agric. Food Chem.* **2000**, *48*, 2040−2043.

(3) Mir, N. A.; Beaudry, R. Effect of superficial scald suppression by diphenylamine application on volatile evolution by stored Cortland apple fruit. *J. Agric. Food Chem.* **1999**, *47*, 7−11.

(4) Du, Z.; Bramlage, W. J. Roles of ethylene in the development of superficial scald in 'Cortland' apples. *J. Am. Soc. Hortic. Sci.* **1994**, *199*, 516−523.

(5) Lurie, S.; Klein, J.; Ben-Arie, R. Physiological changes in diphenylamine-treated 'Granny Smith'. *Isr. J. Bot.* **1989**, *38*, 199−207.

(6) Rudell, D. R.; Mattheis, J. P.; Hertog, M. L. A. T. M. Metabolomic change precedes apple superficial scald symptoms. *J. Agric. Food Chem.* **2009**, *57*, 8459−8466.

(7) Rudell, D. R.; Buchanan, D. A.; Leisso, R. S.; Whitaker, B. D.; Mattheis, J. P.; Zhu, Y.; Varanasi, V. Ripening, storage temperature,

ethylene action, and oxidative stress alter apple peel phytosterol metabolism. *Phytochemistry* **2011**, *72*, 1328−1340.
(8) Galliard, T. Aspects of lipid metabolism in higher plants − II. The identification and quantitative analysis of lipids from the pulp of pre- and post-climacteric apples. *Phytochemistry* **1968**, *7*, 1915−1922.
(9) Magne, C.; Bonenfant-Magne, M.; Audran, J. C. Nitrogenous indicators of postharvest ripening and senescence in apple fruit (*Malus domestica* Borkh. cv. Granny Smith). *Int. J. Plant Sci.* **1997**, *158*, 811−817.
(10) Aprea, E.; Gika, H.; Carlin, S.; Theodoris, G.; Vrhovsek, U.; Mattivi, F. Metabolite profiling on apple volatile content based on solid phase microextraction and gas-chromatograph time of flight mass spectrometry. *J. Chromatogr., A* **2011**, *1218*, 4517−4524.
(11) Carrari, F.; Fernie, A. R. Metabolic regulation underlying fruit development. *J. Exp. Bot.* **2006**, *57*, 1883−1897.
(12) Rudell, D. R.; Mattheis, J. P.; Curry, E. A. Prestorage ultraviolet-white light irradiation alters apple peel metabolome. *J. Agric. Food Chem.* **2008**, *56*, 1138−1147.
(13) Rudell, D. R.; Mattheis, J. P.; Fellman, J. K. Relationship of superficial scald development and α-farnesene oxidation to reactions of diphenylamine and diphenylamine deriviatives in cv. Granny Smith apple peel. *J. Agric. Food Chem.* **2005**, *53*, 8382−8389.
(14) Fischer, E.; Speier, A. Representation of the esters. *Chemistry* **1895**, *28*, 3252−3258.
(15) Chong, I. G.; Jun, C. H. Performance of some variable selection methods when multicollinearity is present. *Chemom. Intell. Lab. Syst.* **2005**, *78*, 103−112.
(16) Xia, J.; Psychogios, N.; Young, N.; Wishart, D. S. MetaboAnalyst: a web server for metabolomics data analysis and interpretation. *Nucleic Acids Res.* **2009**, *37* (Suppl. 2), W652−W660.
(17) Watkins, C. B.; Bramlage, W. J.; Cregoe, B. A. Superficial scald of 'Granny Smith' apples is expressed as a typical chilling injury. *J. Am. Soc. Hortic. Sci.* **1995**, *120*, 88−94.
(18) Huelin, F. E.; Coggiola, M. Superficial scald, a functional disorder of stored apples. V. Oxidation of α-farnesene and its inhibition by diphenylamine. *J. Sci. Food Agric.* **1970**, *21*, 44−48.
(19) Anet, E. F. L. J. Superficial scald, a functional disorder of stored apples. VIII. Volatile products from the autoxodiation of α-farnesene. *J. Sci. Food Agric.* **1972**, *23*, 605−608.
(20) Gapper, N. E.; Bai, J.; Whitaker, B. D. Inhibition of ethylene-induced α-farnesene synthase gene PcAFS1 expression in 'd'Anjou' pears with 1-MCP reduces synthesis and oxidation of α-farnesene and delays development of superficial scald. *Postharvest Biol. Technol.* **2006**, *41*, 225−233.
(21) Rowan, D. D.; Hunt, M. B.; Fielder, S.; Norris, J.; Sherburn, M. S. Conjugated triene oxidation products of α-farnesene induce symptoms of superficial scald on stored apples. *J. Agric. Food Chem.* **2001**, *49*, 2780−2787.
(22) Wojciechowski, Z. A. Biochemistry of phytosterol conjugates. In *Physiology and Biochemistry of Sterols*; Patterson, G. W., Nes, W. D., Eds.; American Oil Chemists' Society: Champaign, IL, 1991; pp 361−395.
(23) Loewus, F. A.; Murthy, P. P. N. *myo*-Inositol metabolism in plants. *Plant Sci.* **2000**, *150*, 1−19.
(24) Moggia, C.; Moya-León, M. A.; Pereira, M.; Yuri, J. A.; Lobos, G. A. Effect of DPA and MCP on chemical compounds related to superficial scald of Granny Smith apples. *Span. J. Agric. Res.* **2010**, *8*, 178−187.
(25) Brummell, D. A. Cell wall disassembly in ripening fruit. *Funct. Plant Biol.* **2006**, *33*, 103−119.
(26) de Vries, J. A.; Voragen, A. G. J.; Robouts, F. M.; Pilnik, W. Changes in the structure of apple pectic substances during ripening and storage. *Carbohydr. Polym.* **1984**, *4*, 3−13.
(27) Fry, S. C.; Dumville, J. C.; Miller, J. G. Fingerprinting of polysaccharides attacked by hydroxyl radicals *in vitro* and in the cell walls of ripening pear fruit. *Biochem. J.* **2001**, *357*, 729−737.
(28) Willats, W.; Orfilia, C.; Limberg, G.; Bucholt, H.; van Alebeek, G. Modulation of the degree and pattern of methyl-esterification of pectichomogalacturonan in plant cell walls. *J. Biol. Chem.* **2001**, *276*, 19404−19413.
(29) Frenkel, C.; Peters, J. S.; Tieman, D. M.; Tiznado, M. E.; Handa, A. K. Pectin methylesterase regulates methanol and ethanol accumulation in ripening tomato (*Lycopersicon esculentum*) fruit. *J. Biol. Chem.* **1998**, *273*, 4293−4295.
(30) Bartley, I. M.; Stoker, P. G.; Martin, A. D. E.; Hatfield, S. G. S.; Knee, M. Synthesis of aroma compounds by apples supplied with alcohols and methyl esters of fatty acids. *J. Sci. Food Agric.* **1985**, *36*, 567−574.
(31) Dixon, J.; Hewett, E. W. Factors affecting apple aroma/flavor volatile concentration: a review. *N. Z. J. Crop Hortic.* **2000**, *28*, 155−173.
(32) Song, J. Flavor volatile production and regulation in apple fruit. *Stewart Postharvest Rev.* **2007**, *3* (2), 1−8.
(33) Mir, N. A.; Wendorf, M.; Pérez, R.; Beaudry, R. M. Chlorophyll fluourescence as affected by some superficial defects in stored apples. *J. Hortic. Sci. Biotechnol.* **1998**, *73*, 846−850.
(34) DeLong, J. M.; Prange, R. K.; Leyte, J. C.; Harrison, P. A. A new technology that determines low-oxygen thresholds in controlled-atmosphere-stored apples. *HortTechnology* **2004**, *14*, 262−266.
(35) Matile, P.; Horstensteiner, S.; Thomas, H. Chlorophyll degradation. *Annu. Rev. Plant Physiol. Plant Mol. Biol.* **1999**, *50*, 67−95.
(36) Knee, M. Anthocyanin, carotenoid, and chlorophyll changes in the peel of Cox's Orange Pippin apples during ripening on and off the tree. *J. Exp. Bot.* **1972**, *23*, 184−196.
(37) Merzlyak, M. N.; Solovchenko, A. E. Photostability of pigments in ripening apple fruit: a possible photoprotective role of carotenoids during plant senescence. *Plant Sci.* **2002**, *163*, 881−888.
(38) Solovchenko, A. E.; Chivkunova, O. B.; Merzlyak, M. N.; Gudkovsky, V. A. Relationships between chlorophyll and carotenoid pigments during on- and off-tree ripening of apple fruit revealed non-destructively with reflectance spectroscopy. *Postharvest Biol. Technol.* **2005**, *38*, 9−17.
(39) Klimov, V. V.; Klievanik, A. V.; Shuvalov, V. A. Reduction of pheophytin in the primary light reaction of photosystem II. *FEBS Lett.* **2002**, *82*, 183−186.
(40) Schwartz, S. J.; Von Elbe, J. H. Kinetics of chlorphyll degradation to phyropheophytin in vegetables. *J. Food Sci.* **1983**, *48*, 1303−1306.
(41) Eckhardt, U.; Grimm, B.; Hortensteiner, S. Recent advances in chlorophyll biosynthesis and breakdown in higher plants. *Plant Mol. Biol.* **2004**, *56*, 1−14.
(42) Kidd, F.; West, C. The production of volatiles by apples: effects of temperature, maturity, technique of estimation. *Rep. Food Invest. Board* **1938**, 136−142.
(43) Azevedo, R. A.; Arruda, P.; Turner, W. L.; Lea, W. L. The biosynthesis and metabolism of the aspartate derived amino acids in higher plants. *Phytochemistry* **1997**, *46*, 395−419.
(44) Sugimoto, N.; Jones, A. D.; Beaudry, R. Changes in free amino acid content in 'Jonagold' apple fruit as related to branch-chain ester production, ripening, and senescence. *J. Am. Soc. Hortic. Sci.* **2011**, *136*, 429−440.
(45) Matich, A.; Rowan, D. Pathway analysis of branched-chain ester biosynthesis in apple using deuterium labeling and enantioselective gas chromatography-mass spectrometry. *J. Agric. Food Chem.* **2007**, *55*, 2727−2735.
(46) Lavilla, T.; Puy, J.; López, M. L.; Recasens, I.; Vendrell, M. Relationships between volatile production, fruit quality, and sensory evaluation in Granny Smith apples stored in different controlled-atmosphere treatments by means of multivariate analysis. *J. Agric. Food Chem.* **1999**, *47*, 3791−3803.
(47) Schaffer, R. J.; Friel, E. N.; Souleyre, E. J. F.; Bolitho, K.; Thodey, K.; Ledger, S.; Bowen, J. H.; Ma, J. H.; Nain, B.; Cohen, D.; Gleave, A. P.; Crowhurst, R. N.; Janssen, B. J.; Yao, J. L.; Newcomb, R. D. A genomics approach reveals that aroma production in apple is controlled by ethylene predominantly at the final step in each biosynthetic pathway. *Plant Physiol.* **2007**, *144*, 1899−1912.

(48) Rowan, D. D.; Lane, H. P.; Allen, J. M.; Fielder, S.; Hunt, M. B. Biosynthesis of 2-methylbutyl, 2-methyl-2-butenyl, and 2-methylbutanoate esters in Red Delicious and Granny Smith apples using deuterium-labeled substrate. *J. Agric. Food Chem.* **1996**, *44*, 3276−3285.
(49) Wooltorton, L. S. C.; Jones, J. D.; Hulme, A. C. Genesis of ethylene in apples. *Nature.* **1965**, *207*, 999−1000.
(50) Ueda, Y.; Ogata, K. Coenzyme A-dependent esterification of alcohols and acids in separated cells of banana pulp and its homogenate. *J. Jpn. Soc. Food Sci. Technol.* **1977**, *24*, 624−630.
(51) Defilippi, B. G.; Manríquez, D.; Luengwilai, K.; González-Agüero, M. Aroma volatiles: biosynthesis and mechanisms of modulation during fruit ripening. *Adv. Bot. Res.* **2009**, *50*, 1−37.
(52) Chervin, C.; Truett, J. K. Alcohol dehydrogenase expression and alcohol production during pear ripening. *J. Am. Soc. Hortic. Sci.* **1999**, *124*, 71−75.
(53) Rowan, D. D.; Allen, J. M.; Fielder, S.; Hunt, M. B. Biosynthesis of straight-chain ester volatiles in Red Delicious and Granny Smith apples using deuterium-labeled precursors. *J. Agric. Food Chem.* **1999**, *47*, 2553−2562.